INFILTRATION IN THE UPPER SPLIT WASH WATERSHED, YUCCA MOUNTAIN, NEVADA

By David A. Woolhiser,[1] Life Member ASCE
Randall W. Fedors[2]
Roger E. Smith,[3] Member ASCE
Stuart A. Stothoff,[4] Member ASCE

Abstract: The KINEROS2 rainfall-runoff model was used to estimate plane and channel infiltration within the Upper Split Wash watershed located above the potential geologic repository for high-level radioactive waste on Yucca Mountain, Nevada. The estimated average annual runoff was 3.6 mm/yr, and the channel and bedrock infiltration rates during storm events were 0.6 and 8.7 mm/yr. Most overland flow was a result of saturation of thin soils during low-intensity winter storms. The spatial distribution of excess infiltration and bedrock infiltration during a rainfall event is dependent on the position within the watershed. Excess infiltration is a positive value when runon leads to infiltration being greater than the local precipitation. The greatest bedrock infiltration occurs on the hillslope areas with thin soils and highest values of bedrock hydraulic conductivity (K_S). The greatest excess infiltration occurs on lower portions of the hillslope with deeper soil depths that receive runoff from upslope areas. A sensitivity study shows that these estimates are most sensitive to soil depth, bedrock K_S, initial water content, and soil water-holding capacity.

[1]Hydrologic Consultant, 2833 Sunstone, Fort Collins, CO 80525, (970) 482-7810; woolhiserd@aol.com

[2]Senior Research Engineer, Center for Nuclear Waste Regulatory Analyses, Southwest Research Institute, 6220 Culebra Road, San Antonio, TX 78238, (210) 522-6818; rfedors@swri.org

[3]Hydrologic Consultant, 819 Columbia Rd., Fort Collins, CO 80525, (970) 492-2662; gedrathsmith@earthlink.net

[4]Principal, Stothoff Environmental Consulting, Winston-Salem, NC 27103, (336) 723-9332; stothoff@bellsouth.net

Keywords: Hydrologic models; catchments; infiltration; percolation; runoff; arid lands; Nevada

INTRODUCTION

Objective

The objective of this study is to utilize the distributed rainfall-runoff model KINEROS2 (Woolhiser et al. 1990, Smith et al. 1995) in conjunction with measured precipitation data to estimate the spatial distribution of storm and mean annual infiltration into soils and bedrock on hillslopes and channels of a small watershed on Yucca Mountain (YM), Nevada. Emphasis is on the impact of the runoff-runon phenomenon on the possible spatial focusing of net infiltration.

Background

Yucca Mountain, Nevada, approximately 160 km northwest of Las Vegas, Nevada, is the potential site of a geologic repository for high-level radioactive waste. The repository would be located approximately 250 m above the water table and within the unsaturated zone (UZ), which is up to 750 m thick. A key criterion for the licensing of the potential repository is whether the engineered and natural barrier systems will meet the performance standards described in the code of Federal regulations 10 CFR Part 63. The quantity of water percolating to the repository horizon has been identified as an important component of the natural barrier system (e.g., Mohanty et al. 2004, EPRI 2002, and BSC 2002). Sources of water fluxes traversing the UZ include percolation below the root zone on upland areas and infiltration in the beds of ephemeral stream channels within the repository footprint. During infrequent surface runoff events, water may be

redistributed from runoff-producing areas to downslope areas with deeper soils or higher saturated hydraulic conductivities (K_S) and to channel alluvium. This redistribution may cause zones of focused infiltration leading to localized deep percolation.

Because of the year-to-year variations of precipitation and wide variations of slope, aspect, soil thickness, and bedrock characteristics in the upland areas, direct measurements alone of water content by neutron probes or other techniques may not provide representative values that can be used to estimate flux reliably. Physically based numerical models of the hydrology, in conjunction with measurements, may provide the best estimates of the present long-term average fluxes. These models provide the only way to estimate deep percolation during hypothesized future climate conditions.

Hydrologic modeling in semiarid environments is extremely difficult because net infiltration and runoff are estimated as the small difference between two relatively large quantities, precipitation and evapotranspiration. One factor especially difficult to handle is the redistribution of water at the ground surface caused by runoff generated over an area that subsequently flows downslope (runon) where it may infiltrate. This phenomenon is most prevalent where there are large variations in hydraulic conductivity of the surface soil or in depth to bedrock or an impeding soil layer (*THICK*). K_S variations should be most significant during high-intensity storms, while variations in soil depth should be important during long-duration, low-intensity storms. To help describe the spatial redistribution of surface waters and its effect on infiltration, the term effective precipitation is used. Effective precipitation is defined as the local precipitation adjusted for runoff and runon and, thus, is the water available for local infiltration. The runoff/runon phenomenon results in some areas having below-average effective precipitation

(runoff), while other areas receive an above-average effective precipitation (runon) that may lead to positive values of excess infiltration (infiltration greater than local precipitation). These differences will, in turn, affect the vegetation and the flux of water to the atmosphere.

The KINEROS2 Version 1.12 watershed model (Woolhiser et al. 1990, Smith et al. 1995) is used in this report for estimating runoff, runon, and infiltration on a small watershed near the crest of Yucca Mountain, Nevada. The KINEROS2 model was previously used to estimate runoff in Solitario Canyon, a larger watershed that encompasses the west slope of YM and the adjacent valley (Woolhiser et al. 2000). Two other approaches have also been used to estimate spatially dependent net infiltration at YM. The INFIL model (USGS 2001, Hevesi et al. 2003) has been used to estimate net infiltration, though the estimates cover the entire YM area. INFIL is a daily water balance model that includes evapotranspiration and surface water routing on a 30-m × 30-m grid. It was developed to estimate average net infiltration rates over long time periods (e.g., 10,000 yr). In another approach, the Richards equation solver in the one-dimensional BREATH code (Stothoff 1995) was used to estimate net infiltration for an appropriate range of possible conditions and parameters for YM. These results were then linked to a regular grid, with each element containing local characteristics, to estimate spatial variations in net infiltration for the entire YM area (Mohanty et al. 2002). Methods to constrain net infiltration models or to provide independent estimates of net infiltration are described in Flint et al. (2001) and include the use of neutron probes, thermal profiles, chloride mass balance, atmospheric radionuclides, and empirical relations.

Climate

The climate of YM is controlled by the interaction of weather systems with major topographical features of the region. In winter, most of the weather systems providing moisture to this area of the desert southwest originate in the Pacific Ocean. Precipitation occurs in the Sierra Nevada Mountains to the west, producing a rain shadow over YM. Moisture during the summer comes from the south and southeast and is carried by southerly winds that curve to the east in the YM area. French (1983) identified three precipitation zones in southern Nevada: a deficit zone within the rain shadow, an excess zone southeast of the rain shadow, and a transition zone between them. YM is within the transition zone. The average annual precipitation at Upper Split Wash is estimated to be 181 mm. Precipitation varies seasonally, with a summer maximum in August and a winter rainfall period extending from October through April. The summer rainfall may occur as thunderstorms with high intensities, while winter rainfall has lower intensities and longer durations. Winter snow accumulation is minimal for the modern climate.

Watershed Description

The 0.25 km^2-Upper Split Wash watershed lies over the proposed repository with elevations ranging from 1,301 m at the mouth of the watershed to 1,478 m at Yucca Crest. A topographic map of YM including streamgage and raingage locations is shown in Figure 1. Stream channels incised into bedrock, alluvium, and paleo-terrace deposits flow only during or immediately after precipitation events. Bedrock geology has been described by Day et al. (1998) and consists of five lithostratographic units of Tiva Canyon Tuff. Hillslopes are steep, and soils are generally thin and very rocky, with areas of bare rock. Soil depths on the gently sloping

ridgetops are more uniform than on the steep sideslopes. Soil depths generally range from 0- to 1-m thick (Mohanty et al. 2002) based on field investigations and a mass balance model. Channels are narrow (1–3 m wide) with highly variable amounts of alluvium ranging from zero to several meters thick. The eastern extent of the channel contains remnants of terrace deposits and thick alluvium. Vegetation consists primarily of shrubs typical of the transition zone between the northern boundary of the Mojave Desert and the southern boundary of the Great Basin Desert (USGS 2001). Plants are frequently subjected to stress because of the large variability of precipitation and water availability as affected by soil depth and the runoff-runon phenomenon.

KINEROS2 MODEL

The KINEROS2 model, an improved version of KINEROS (Woolhiser et al. 1990), is described in detail by Smith et al. (1995). It is a distributed model, with hillslope features described as cascades of planes contributing flow to channels either as concentrated flow at the upper boundary or as uniformly distributed lateral flow. Rainfall rates are obtained by differencing the accumulated rainfall function and may be specified independently for each element by interpolation between raingages. The Smith-Parlange equation (Smith and Parlange 1978) is used to describe the interactive infiltration at each computational node on both plane and channel elements. Small-scale spatial variability is accommodated by assuming that the saturated hydraulic conductivity is log-normally distributed and is specified by the mean and the coefficient of variation (Smith et al. 1990, 1995). If there is a rainfall hiatus during which drying can occur near the surface, the redistribution of soil water is handled by a method described in Smith et al. (1993) and Corradini et al. (1994). Two soil layers (or soil and bedrock) can be specified for

plane and channel elements. Surface runoff can be generated when rainfall rates exceed the infiltrability of the soil (Hortonian mechanism) or can be induced when the top layer becomes saturated (saturation-induced mechanism). Overland and channel flows are described by the one-dimensional kinematic wave equations solved by finite difference techniques. The KINEROS model has been thoroughly tested over a range of catchment sizes in a semiarid environment where only Hortonian runoff occurred (Goodrich 1990). KINEROS2 uses the same fundamental equations as KINEROS.

Watershed Geometry and Model Parameters

The plane and channel network required by the KINEROS2 model was derived from a 10-ft contour interval topographic map from Day et al. (1998). Channel reaches were first designated based upon relative uniformity of channel cross sections, slopes, depths of alluvium, and type of bedrock as determined from topographic and geologic maps and from field investigations. To mark the edges of plane elements, flow lines were drawn at right angles to the topographic contour lines beginning at the upper and lower ends of the channels. Topographic, geologic, and soil depth maps linked by a geographic information system (GIS) facilitated further subdivision of plane and channel elements. In the GIS framework, plane and channel elements were revised such that the slope, bedrock type and soil depth were well defined by the network. Shown in Figure 2 with the bedrock geology is the model grid with 196 plane (black lines) and 20 channel (blue lines) elements. The length-weighted average plane and channel slopes were 0.33 and 0.24; the latter is high because of steep sections of the channel at the headwall of the valley.

In the KINEROS2 model, channel cross sections are trapezoidal defined by a bottom width, *BW*, and side slopes, *SS*1 and *SS*2. One channel was modeled as a compound channel with additional parameters representing the overbank section: width, slope, elevation difference between the overbank and the channel bed, and side slope. All channel cross-sectional parameters were estimated from field measurements, and slopes were determined from the topographic map. The actual channels are irregular and rough, with large rocks obstructing the flow. Although calculations of flow in a trapezoidal channel may not represent the local flow details, the approximation is considered adequate in an average sense.

The average length of the Δx increments in the finite difference form of the kinematic wave equations was 3.6 m. The computational time increments were 2 min.

Parameters and Initial Conditions

Subgrid variations for all soil and bedrock properties are accounted for in this model by the use of representative property values. Soil thickness and percent bedrock exposure strongly vary, even at the submeter scale. Soil depth values for plane elements were estimated visually from a color-coded map developed using soil depth data from Mohanty et al. (2002).

The saturated hydraulic conductivities of surface soil and bedrock are critical parameters in partitioning rainfall between Hortonian overland flow, infiltration into the soil, and percolation into bedrock. K_s values for undisturbed soils were the same as those used by Woolhiser et al. (2000), specifically 22.25 mm/hr for the period December–June and 11.25 mm/hr for –November. These values were determined by an analysis of rainfall simulator data from plots near Mercury, Nevada on the Nevada Test Site (NTS). Procedures for the rainfall simulator studies are described

by Simanton et al. (1986), and a summary of the data collected is published by Lane (1986, Appendix A). The specific seasonal variations used here were based on the hypothesis that the variations were caused by winter freeze-thaw processes and the subsequent compaction by summer rains.

The geometric representation of Upper Split Wash has a resolution that requires K_s values for areas disturbed by roads and other activities. In those areas, near Yucca Crest, the vegetation has been removed, and the soil has been compacted by traffic. Based on rainfall simulator runs on bare plots (Simanton et al. 1986), a K_s value of 1.9 mm/hr was chosen and assigned to planes 3, 4, 5, 6, 7, 8, 16, 17, 18, 27, 28, 40, 41, 55, 74, 81, and 88 (Figure 2). The reduction in K_s will result in increased Hortonian runoff from the disturbed areas and an increase of infiltration for downstream elements.

K_s values for the bedrock range between 0.35 and 0.68 mm/hr for the Tiva Canyon units (Figure 2) based on estimates presented by Flint et al. (1996), which are an order of magnitude larger than those presented in USGS (2001). These estimates reflect bulk properties of the matrix and fracture network. The plane element boundaries were chosen to conform with the bedrock units in addition to changes in slope and hillslope convergence or divergence, so the conductivities were readily assigned. Bedrock K_s for channels was assigned in the same manner. K_s for channel alluvium was set at 61 mm/h based on textural estimates and Table 2 of Woolhiser et al. (1990). The coefficient of variation (CV) of K_s was set at 0.8 for all plane elements, the same value used by Woolhiser et al. (2000) and based upon work by Goodrich (1990).

The net capillary drive parameter, G, was set at 50 mm for undisturbed areas, the same value used by Woolhiser et al. (2000). For disturbed areas it was set at 80 mm, based on the

rainfall simulator data for the bare plots at Mercury, Nevada. Bedrock *G* was set at 60 mm, while the *G* for channel alluvium was set at 63 mm. The parameter λ (herein called *DIST*) in the Brooks-Corey soil water function (Brooks and Corey, 1964) was estimated from soil textural information.

The soil porosity, *POR*, was set at 0.34 based on measurements by Lane et al. (1984) in Rock Valley in the NTS. This value is consistent with a value of 0.39 determined from an analysis of field data from YM presented by Schmidt (1988). Bedrock porosity was set at 0.20.

In KINEROS2, lateral microtopographic variations on hillslopes are represented as parallel triangular sections with mean values of relief (*RE*), depth in millimeter, and spacing (*SPA*), the distance in meters between crests or bottoms of these channels. Woolhiser et al. (2000) found that runoff was insensitive to the spacing, so *SPA* was set at 1 m. *RE* was set at 50 mm for elements near the top of the slope, 100 mm for planes at midslope, and 150 mm for elements at the toe of the slope. The increase in *RE* downslope is consistent with the idea that the depth of rills increases in the downslope direction. The *RE* parameter determines the relative area covered by water, defined for each computational node on a plane when the rainfall rate falls below the infiltrability or when runon is occurring

Initial relative soil saturation, *SAT*, varied seasonally based on monthly averages measured over a 5-yr period at nearby Rock Valley (Lane et al. 1984). *SAT* was set at 0.325 for January–April, 0.155 for June–October, and 0.235 for November–December. The soil water profile was represented as a step function with relative saturation from the surface to a depth determined by the 7-day antecedent precipitation (*API*). The maximum relative soil saturation allowed in KINEROS2 is 0.95 to reflect entrapped air during imbibition. Bedrock *SAT* is

calculated internally in KINEROS2 such that the suction at the interface matches that for the soil with the specified initial relative saturation. *SAT* of channel alluvium was set at 0.13, corresponding to permanent wilting for a loamy sand.

Field observations and photographs were used to estimate Manning's *n* for plane and channel elements. The value of 0.151 for planes is within the range of data presented by Weltz et al. (1992) for brush lands in the Mojave Desert. Manning's *n* for channels was set at 0.0651 based on information in Table 6-1 in Simons, Li and Associates (1982), and is the same value used by Woolhiser et al. (2000) for first-order channels in Solitario Canyon, west of YM.

Precipitation Data

Tipping bucket raingage data were available for some nearby gages for a relatively short period of record. These data were collected by the U.S. Geological Survey (USGS) and Science Applications International Corporation (SAIC) and are available from the YM Project, U.S. Department of Energy. Gage USGS WX-3 covered the period September 1988–August 1994 and gages SAIC #8 and SAIC #18 covered the period October 1994–September 1996. Although gage SAIC #18 is the nearest of the SAIC gages to Upper Split Wash, data were missing for the period from February 16 to April 20, 1995. A major rainfall event occurred during this period, so data from gage SAIC #8 were used for the storm of March 9–11, 1995.

Because KINEROS2 is an event-based model and the objective of the study is to examine the effects of runoff-runon on deep percolation, it was necessary to select rainfall events that could cause either Hortonian or saturation-induced overland flow. The records were first examined to determine summer rainfall events greater than 12.7 mm or winter events with more

than 25.4 mm in a 3-day period. These events were then examined to determine if the intensity was great enough to cause Hortonian runoff, given the seasonal K_S, or if the depth of rainfall was great enough to cause saturation of the plane element with the thinnest soil given the seasonal initial water content. Events meeting these criteria are listed in Table 1.

SIMULATION OF PLANE AND CHANNEL INFILTRATION AND RUNOFF

There are two runoff-generating mechanisms in the Upper Split Wash watershed. The Hortonian mechanism, in which the rainfall rate must exceed the infiltrability (sometimes called infiltration capacity) of the soil, would usually occur in the summer and fall as a result of thunderstorm rainfall, but could occur throughout the year from the disturbed portions of the watershed. The saturation-induced mechanism would occur during the winter when the rainfall depth is great enough to saturate soil layers upward from the bedrock interface, particularly common where the soils are thin.

The KINEROS2 output file for each storm displays the total volume of infiltration for each plane and channel element in m^3 and in mm expressed over the entire watershed. If the plane or channel element becomes saturated during the event, it includes the depth of infiltration required to saturate the element and the time from the beginning of the event when saturation occurred. The spatial distribution of infiltration can be described concisely by calculating the cumulative distribution function (CDF) with respect to area of infiltration depth and excess infiltration (i.e., the infiltration depth for each plane minus the rainfall).

If, for the i^{th} plane element for the j^{th} storm, we denote the depth of infiltration by f_{ij} and the rainfall depth by $P_{ij,}$ the excess infiltration is given by the expression

$$e_{ij} = f_{ij} - P_{ij} \tag{1}$$

The total excess infiltration for m storms in N years for plane i is then

$$E_i = \sum_{j=1}^{m} e_{ij} = \sum_{j=1}^{m} (f_{ij} - P_{ij}) = \sum_{j=1}^{m} f_{ij} - \sum_{j=1}^{m} P_{ij} \tag{2}$$

The average annual excess for plane i for N years is

$$\overline{E}_i = E_i / N \tag{3}$$

A positive excess indicates that there is runon from an upslope plane, and a negative excess indicates that there is runoff from the plane. Negative excess will be observed for planes with thin soils that saturate during rainfall events or for planes with low values of K_S such as roads.

When saturation-induced runoff is occurring, the quantity infiltrated will depend upon the hydraulic conductivity of the bedrock and the storm duration. Infiltration into the bedrock of plane i for storm j, F_{Bij} is the total flux passing across the soil–bedrock interface during the calculated storm period. Infiltration into bedrock may occur after the storm ends, but will be affected by evapotranspiration and downslope saturated and unsaturated flow in the soil layer. The potential bedrock infiltration, F_{BPij}, is defined as the sum of bedrock infiltration during the storm and the quantity of water held in soil water storage that could drain by gravity into the bedrock.

Net infiltration that continues as deep percolation is water that moves below the reach of evapotranspiration. Generally at YM, evapotranspiration is prominent in the periods after storms. Also, the root zone depth where soils are thin likely extends into the bedrock. Bedrock infiltration as used in this report may closely represent net infiltration, although when climatic conditions

allow, net infiltration will likely be between the values of bedrock infiltration and potential bedrock infiltration.

Plane and Bedrock Infiltration

The KINEROS2 model was run with all the rainfall events listed in Table 1, which also provides a summary of the corresponding results. For this 9-yr period, the KINEROS2 model estimated mean annual runoff, channel infiltration, bedrock infiltration, and potential bedrock infiltration of 3.6, 0.6, 8.7, and 48 mm/yr, respectively. Large storms such as those that occurred in January and March of 1995 (S8_3995b and S18_95_2) are infrequent but account for much of the deep percolation. Although these storms are the largest in the YM rainfall data set used in this study, their maximum intensities are nearly a factor of five lower than the intensity associated with the 100-yr return runoff event noted in Woolhiser et al. (2000). The CDFs of plane and bedrock infiltration for the events G3_88_1 and S8_3995b are shown in Figure 3. The excess infiltration on about 70% of the watershed was negative for the larger event, indicating runoff induced by saturation of thin soils. Excess infiltration was greater than 10 mm on approximately 15% of the watershed, showing that runon was significant. The CDF of bedrock infiltration (dashed curve in Figure 3) shows that approximately 79% of the watershed had infiltration through the soil–bedrock interface during the event and that for approximately 18% of the area infiltration was greater than 20 mm. The CDF of potential bedrock infiltration (short dashed curve in Figure 3) shows that potential infiltration for approximately 95% of the watershed greater than zero and was greater than 50 mm for 50% of the area. The upper tail of the CDFs represents channel elements that have large amounts of infiltration, but occupy a small portion of the watershed area. The rainfall

hyetograph and the runoff hydrograph at the mouth of the watershed for this event are shown in Figure 4. After 1,550 min, the hydrograph pattern is very similar to the hyetograph, reflecting saturation-induced overland flow with an increase of the saturated area as the storm continues.

CDFs of the 9-yr averages of excess infiltration, bedrock infiltration, and potential bedrock infiltration for all elements are shown in Figure 5. Bedrock infiltration and potential bedrock infiltration for three slope classes and the channel elements are shown in Figure 6. The relative areas of the slope classes are ridge = 29.95%, slope = 59.6%, toe of slope = 9.77%, and channel = 0.68%. Figures 5 and 6 demonstrate the extreme spatial variability of bedrock infiltration. Although the 9-yr average bedrock infiltration is 8.7 mm/yr, 75% of the ridge elements have greater than the average value and approximately 50% of the ridge area has bedrock infiltration greater than twice the average. Approximately 25% of the channel area has more than three times the watershed average bedrock infiltration.

Figure 5 shows that approximately 32% of the watershed area receives more than the rainfall for these runoff-producing storms and approximately 8% of the area has an average excess infiltration greater than 5 mm/yr. This redistribution of rainfall could significantly affect vegetation and deep percolation. If the excess infiltration is not sufficient to saturate the soil and the vegetation type and density adapt to the added moisture, percolation below the root zone may be very infrequent or may not occur at all in deep soils. Figure 5 also reveals that potential bedrock infiltration occurred over nearly 95% of the watershed area at some time during the 9-yr period. The median annual potential bedrock infiltration was 59 mm/yr, greater than the mean value of 48 mm/yr.

Channel Infiltration

Water infiltrates into channel alluvium during runoff events. If the alluvium is thin, the water may be impeded by the bedrock with a K_S much smaller than that of the alluvium. A typical channel cross section as modeled by KINEROS2 is shown in Figure 7. When runoff is in the channel, infiltration is modeled by the Smith-Parlange model (Smith and Parlange 1978) with an effective infiltrating wetted perimeter given by the following equation

$$P_e = \max\left[\min\left\{ h \Big/ 0.0856\sqrt{BW}, 1\right\} P_w, 0.05BW\right] \tag{4}$$

where P_e is the effective infiltrating wetted perimeter, h is the depth of flow in the trapezoidal channel, P_w is the wetted perimeter, and BW is the bottom width. Thus the minimum effective infiltrating wetted perimeter is 5% of the bottom width and, when $h > 0.0856\ BW^{0.5}$ the effective width is the same as the wetted perimeter. This function was developed to reduce infiltration rates in channels with a large BW and with deep alluvium. During those conditions, the one-dimensional Smith-Parlange equation is appropriate. A problem arises, however, when this relationship is used for narrow channels with thin alluvium as are found in Upper Split Wash. For low-intensity winter storms that cause saturation-induced overland flow, the flow rate is small so P_e is a small fraction of P_w. The one-dimensional front of infiltrating water detects the bedrock and the infiltration rate is reduced to bedrock K_S. The alluvium does not become saturated over the entire bottom width of the channel. In reality, two-dimensional porous media flow would allow the effective infiltration rate to remain relatively high until the channel alluvium was saturated. Also, rain falling on the channel may saturate the thin alluvium. KINEROS2 has an option that allows

infiltration to occur over the entire hydraulic wetted perimeter of the trapezoidal channel. The channel infiltration using this option should provide an approximate upper bound. This option was activated for this study. Channel infiltration shown in Table 1 is expressed as depth in millimeter over the entire watershed. The channel area is 0.68% of the watershed area, so the average channel infiltration during runoff is approximately 85 mm/yr.

Mean annual channel infiltration shown in Table 1 is based upon calculations for the duration of each storm. Some of this water may infiltrate into the underlying bedrock during a storm, but this is an underestimate of deep percolation because bedrock infiltration would continue until the overlying soil or alluvium desaturates. As a first approximation, it is assumed that water in the channel alluvium will drain into bedrock until the alluvium reaches field capacity. This quantity, which can be called potential channel bedrock infiltration, was calculated for each channel for each storm. The volumes were then summed and averaged for each channel, and the CDFs were computed based upon the surface areas of the channels. The CDFs for the 9-yr averages are shown in Figure 8. The figure reveals that there is potentially much more infiltration into bedrock if it is assumed that the channel alluvium will drain to field capacity. Channel 115 had the greatest annual average excess infiltration (49 mm/yr) and potential bedrock infiltration (119 mm/yr), but averaged only 4.3-mm/yr bedrock infiltration during storms. This low average reflects the thickness of the alluvium for this channel. The bedrock in channel 115 is Tcpll with K_s of 0.418 mm/hr. Assuming that the average is a single event, it would take a minimum of 274 hr after the storm ended for the alluvium to drain into bedrock if it were purely one-dimensional flow and evapotranspiration were assumed negligible. The actual flow pattern is more complicated because there would be lateral flow at the soil–bedrock interface and flow into bedrock fractures,

so the flow patterns would be three-dimensional. Potential bedrock infiltration, which is the same as bedrock infiltration during storms for channels on bedrock, and ranges from 33 to 39 mm/yr and is controlled by the duration of rainfall and runoff. Although the potential infiltration rate below individual channels is large and could affect the interpretation of tracer studies, its volume is small compared with hillslope infiltration because of the relatively small channel area.

COMPARISON OF MODEL RESULTS WITH MEASUREMENTS AT NEARBY WATERSHEDS

USGS has streamgaging stations on some small watersheds near Upper Split Wash (Pabst et al. 1993, Kane et al. 1994). Information for these stations is presented in Table 2. Because no runoff measurements were taken at the outlet of Upper Split Wash during the time period studied, the accuracy of the model with regard to runoff volumes and peak rates is unknown. However, by comparing model results with measurements for the stations shown in Table 2, it is possible to judge if the results are reasonable. USGS records indicate that there was no runoff at Pagany Wash #1 during 1993 and 1994. Model results show no runoff for two potential runoff-producing storms in 1993 and no runoff for one storm in 1994. USGS records showed two runoff events in 1995 (USGS 1995), which agree with model results. Runoff rates and volumes are compared with model results in Table 2.

For the storm of March 9–11, 1995 (S8_3995b), the modeled unit volumes and peak rates are intermediate between those of the nearby stations, suggesting that the model results are reasonable. Gage SAIC #8 is north of Upper Split Wash, and the rainfall gradient for this storm was increasing from south to north as indicated by gages south and east of the watershed. It is

likely that the total rainfall for this storm was less than 80.3 mm, possibly as much as 15–20 mm less. Estimated runoff peaks and volumes are higher than the measured rates downstream at Quac Canyon, which is consistent with the relationship between the same quantities for the two stations on Pagany Wash. The higher runoff per unit area for the smaller watersheds may result from rainfall gradients caused by the convective nature of the storm, from thin soils in the smaller watersheds, or from greater infiltration in the channel alluvium of larger watersheds.

For the storm of January 25–26, 1995, the modeled runoff is much higher than that at nearby stations. Rainfall data at gage SAIC #18 were 87 mm and at gage SAIC #8 were 85 mm. The rainfall at Upper Split Wash could not have been very different. This event was a 6-day storm with low intensities, so runoff would have been a result of saturation-induced overland flow. The runoff volumes published by USGS were estimates except for Wren Wash, which had a runoff of slightly more than half of the modeled runoff. Several possible reasons for the difference include too high *SAT* or *API*, too thin soil depths, and underestimates of bedrock K_s in the model. The relative importance of these factors can be judged by reviewing the sensitivity analysis in the next section.

All the significant runoff events analyzed earlier occurred in the winter season; however, runoff can occur from summer convective thunderstorm rainfall. For example, on July 23, 1984, a peak flow of 34.8 mm/hr was estimated at Split Wash at Quac Canyon (Pabst et al., 1993). This discharge is much higher than the peak rates estimated from maximum stage gages on small watersheds during a 15-yr period (CRWMS M&O 2000, Table 7.1-2) and is near the 100-yr event for watersheds of this size as estimated by Squires and Young (1984). The simulated rainfall events that led to the 10- and 100-yr peak runoff rates reported by Woolhiser et al. (2000) were

used as input to the Upper Split Wash model. The 10-yr storm SEP5A.PRE resulted in a peak rate of 9.1 mm/hr, runoff volume of 6.7 mm and channel infiltration of 0.62 mm. The peak rate is reasonable when compared with peak stage data obtained from small watersheds in the area (CRWMS M&O, 2000). The 100-yr storm PAUG4.PRE resulted in a peak rate of 37 mm/hr, a volume of 12 mm and channel infiltration of 1.1 mm. This peak rate is consistent with that rate cited by Pabst et al. (1993) and appears to be near the value from the Squires and Young (1984) 100-yr peak rate. The area of Upper Split Wash, however, is smaller than any of the watersheds evaluated by Squires and Young (1984). The peak flow rate is higher than rates for a similar sized watershed modeled by Woolhiser et al. (2000), possibly reflecting the effect of the disturbed area in the Upper Split Wash watershed. All runoff for these two storms is attributed to the Hortonian mechanism. None of the plane elements became saturated, although the channel alluvium did. Because of the higher flow rates and resulting larger wetted areas, the channel infiltration was greater than for the winter storms. It is unlikely that this summer runoff on such a small watershed would cause deep percolation because of the actively transpiring vegetation in the narrow channels. Runoff transmitted to wider channels downslope of the model domain, however, could penetrate into the deep alluvium beyond the reach of evapotranspiration and percolate into the bedrock.

SENSITIVITY ANALYSIS

There are many sources of error in hydrological modeling, including input, model and parameter errors. In this study, the primary inputs are rainfall data and initial soil water content. Model error is associated with the structure of the model and algorithms used to describe the

physical processes involved. Parameter error refers to uncertainties in estimating the parameters included in the model equations.

The SAIC and USGS precipitation data were measured with tipping bucket raingages. None of the raingages used (USGS WX-3 and SAIC #8 and #18 in Figure 1) is located within the watershed. The inherent assumption is that these rainfall data are equally likely to have occurred over the watershed during a similar time interval. Other uncertainties include raingage errors, spatial variability of rainfall, editing errors, and representativeness of the observed rainfall sequences. Tipping bucket raingages are known to underestimate rainfall during very intense storms. This error is probably not serious because no high-intensity storms were observed. Underestimation of precipitation may also occur during snowstorms and when precipitation is accompanied by high winds.

The assumption of spatial uniformity of rainfall undoubtedly introduces error. This error would be most serious during summer thunderstorms. Only three storms were in this category, and they were not very intense. The tipping bucket rainfall data were manually edited to isolate periods of rainfall that could potentially cause Hortonian or saturation-induced overland flow. Some data points were eliminated from the record of these storms to reduce the volume of data. This elimination would cause a slight variation in the intensity pattern, but is not considered to be significant for saturation overland flow, because the total depth of the storm was always preserved. The greatest source of uncertainty regarding annual average excess infiltration is probably a result of the short record (9 yr). Precipitation is highly variable in arid regions, and averages of precipitation and any functions of precipitation for this short period of time have large variances.

Model errors are difficult to evaluate unless model results can be compared with detailed measurements of soil water content, surface runoff, and deep percolation. The primary algorithms in the KINEROS2 model have been thoroughly tested on a semiarid watershed where the runoff is generated by the Hortonian mechanism. The model performed well for catchments up to 6.3 km^2 (Goodrich 1990). The program has not been tested against experimental measurements where the runoff mechanism is saturation-induced overland flow.

The representation of a watershed such as Upper Split Wash as a cascade of planes and channels is a severe abstraction. The fidelity of the representation is dependent on the accuracy of the topographic and geologic maps used to outline plane and channel elements. The map used had a 10-ft contour interval so geomorphic factors such as the CDF of elevation, the drainage density, average length of overland flow, and concavity or convexity of slopes should be reasonably accurate. Average soil depth for each plane element was estimated visually from a color-coded map, which, in turn, was based a on model used in Mohanty et al. (2002) in conjunction with field observations. Spatial variations of soil depth occur within plane elements and cannot be accounted for.

A thorough sensitivity study of the KINEROS2 model was made for the Upper Split Wash watershed. Woolhiser et al. (2000) completed a sensitivity study for the nearby Solitario Canyon watershed. They did not model thin soils, however, so all runoff from their simulated storms was generated by the Hortonian mechanism. For the largest storms used as input in this study, runoff was caused by saturation-induced overland flow over a substantial portion of the watershed. Hortonian runoff occurred only from the disturbed areas. Infiltration into soil and bedrock should be most sensitive to parameters that affect the portion of the area that becomes saturated and the

duration of saturation, such as soil depth, initial relative saturation, and bedrock K_S. The potential bedrock infiltration should be sensitive to the same parameters as well as soil water-holding characteristics.

Two storms were used as input, S8_3995b and G3_88_1 (see Table 1). The first storm had a moderate precipitation depth and a low antecedent precipitation index. The second storm had a large precipitation depth and a high antecedent precipitation index. A dimensionless sensitivity coefficient, S, was calculated by the relationship

$$S = \frac{\Delta F}{\Delta P}\frac{P}{F} \tag{5}$$

where ΔF is the change in the output function F resulting from the perturbation ΔP of the parameter P. If the absolute value of S is greater than one, it means that parameter error is magnified, and the results are sensitive to that parameter. A perturbation of $\Delta P = 0.2P$ was used (i.e., a 20% increase). The following sensitivity coefficients were calculated:

1. S_V, sensitivity of runoff volume
2. S_{CF}, sensitivity of total channel infiltration
3. S_{QP}, sensitivity of peak runoff rate
4. S_{FB}, sensitivity of median bedrock infiltration
5. S_{FBP}, sensitivity of median potential bedrock infiltration

Sensitivities of KINEROS2 outputs were obtained by perturbing only one parameter or watershed descriptor at a time. This procedure ignores possible interactions that may exist in this complex nonlinear model.

Values for sensitivity coefficients shown in Table 3 indicate that runoff and infiltration are highly sensitive to a 20% increase in the depth of soil and channel alluvium (*THICK*). Increasing *THICK* of planes and channels decreased the volume of runoff, resulting in negative values of S_V and S_{QP}. The large sensitivity coefficients for G3_88_1 reflect the effect of a small runoff volume (0.02 mm for the reference case) that was near a threshold. Sensitivity coefficients for channel infiltration are positive for the two storms. The channel alluvium was saturated for all channels for the reference case, so increasing the channel *THICK* results in a longer time before the infiltration rate is controlled by the bedrock hydraulic conductivity. Consequently, there is more infiltration into the soil.

Sensitivity coefficients for bedrock K_S, *API, DIST*, and *G* are generally less than those for soil thickness. Increasing the bedrock K_S results in less runoff and lower peak rates for both events (Table 3) and increased channel infiltration and potential bedrock infiltration. Net infiltration is sensitive to bedrock hydraulic conductivity when soils are thin but still present. Where little or no soil is present, most of the precipitation is converted to runoff before infiltration can occur. Where thick soils are present, infiltrating water cannot pass beyond the reach of evapotranspiration for most storms. In a large-scale infiltration field test northeast of Upper Split Wash (BSC 2003), applied surface fluxes suggest that bulk bedrock K_S may be underestimated by one to two orders of magnitude from that in USGS (2001) and by a factor of two from those used in this paper. Sensitivity coefficients for perturbation of the *API* are larger for the smaller storm, which may reflect the large relative increase for low *API* storms. Increasing the soil hydraulic parameter, *DIST*, which defines the field capacity and the wilting point, results in decreases in runoff and peak flow and slight decreases in channel infiltration. Again, sensitivity was greatest for the

smaller storm. Bedrock infiltration was increased for both storms, reflecting the runoff decrease. Sensitivity coefficients were insensitive to the capillary drive parameter, *G*. This appears reasonable because rainfall intensities were low and runoff was caused by the saturation-induced mechanism.

CONCLUSIONS AND RECOMMENDATIONS

The KINEROS2 model was used to model infiltration and runoff for the Upper Split Wash watershed for 18 potential runoff-producing rainfall events measured at nearby raingages during a nine-year period. The following conclusions appear to be justified by the analysis.

Simulations with 18 storms during a 9-yr period show that approximately 28% of the watershed area receives runon such that infiltration exceeds local precipitation and approximately 3% of the area has an average excess infiltration greater than 5 mm/yr. Runoff was generated almost exclusively by the saturation-induced mechanism. The redistribution of rainfall caused by the runoff-runon phenomenon could significantly affect vegetation and deep percolation. The average annual runoff was 3.6 mm/yr, which is greater than the runoff estimated by Woolhiser et al. (2000) for an average plane element in the nearby Solitario Canyon watershed. However, the range of runoff (0.38–1.5 mm/yr) estimated by Woolhiser et al. (2000) was generated only by the Hortonian mechanism. The 10 km^2 Solitario Canyon watershed model, however, neglected soil depth and is larger than the Upper Split Wash watershed; note that runoff decreases with watershed area in arid regions.

The average annual channel infiltration for runoff-producing events was 0.58 mm/yr expressed as depth over the watershed and 84.9 mm/yr expressed as depth over the channel bed

area. The mean annual potential bedrock infiltration for the watershed was 47.6 mm and the median for all channels was 92 mm/yr (range from 8 to 119 mm/yr), either of which are greater than the 10-mm/yr recharge based on an estimate of percolation flux for nearby Pagany and Drillhole Washes (Kwicklis and Rousseau 1999). This difference should be expected because Pagany and Drillhole Washes have deeper channel alluvium than Upper Split Wash and, in this study, evapotranspiration subsequent to each storm is ignored. The values calculated for Upper Split Wash may be overestimates because the option that infiltration occurred over the entire width of the channel bottom was used. Deep percolation into bedrock below channels for small watersheds appear to be relatively small compared to ridge and hillslope infiltration because the relative area of the channels is small. However, there is a significant concentration of potential bedrock infiltration in channels, which can affect the interpretation of radioisotope tracer analyses.

Bedrock infiltration and runoff volume showed the greatest sensitivity to the soil and alluvium depth, *THICK*, with the highest sensitivities for the smaller storm. The potential bedrock infiltration was most sensitive to *DIST* for the larger storm and to *THICK* for the smaller storm, but the sensitivity coefficients were less than 1. The considerable variations in soil depths and topographic features within any plane element modeled would result in an undetermined amount of spatial variability of bedrock infiltration within each element. Sensitivity coefficients of runoff volume and peak rates to *API* were moderate for the smaller storm but relatively small for the large storm.

Channel infiltration was most sensitive to the depths of soil and channel alluvium. Soil depth has a large effect on runoff volume generated by the saturation-induced mechanism and

subsequently reaching the channels. The depth of channel alluvium determines the channel infiltration required for saturation to occur.

Future analyses of evapotranspiration and bedrock percolation in the long periods between storms should improve estimates of deep percolation when incorporating the runoff and excess infiltration estimated using the event-based KINEROS2 program.

ACKNOWLEDGMENTS

This paper was prepared to document work performed by the Center for Nuclear Waste Regulatory Analyses (CNWRA) for the U.S. Nuclear Regulatory Commission (NRC) under Contract No. NRC–02–02–012. The activities reported here were performed on behalf of the NRC Office of Nuclear Material Safety and Safeguards, Division of High-Level Waste Repository Safety. This paper is an independent product of CNWRA and does not necessarily reflect the view or regulatory position of NRC.

The authors thank D.C. Goodrich and C. Unkrich of the Agricultural Research Service, U.S. Department of Agriculture, for their assistance with the KINEROS2 model.

Appendix I. References

Brooks, R.H., and Corey, A.T. (1964). *Hydraulic properties of porous media.* Hydrology Paper 3. Colorado State University, Fort Collins, Co.

BSC. (2002). *Risk information to support prioritization of performance assessment models.* TDR–WIS–PA–+000009, Rev 01 ICN01. Bechtel SAIC Company, LLC, Las Vegas, Nv.

BSC. (2003). *In situ field testing of processes.* ANL–NBS–HS–000005, Rev 02. Bechtel SAIC Company, LLC, Las Vegas, Nv.

Corradini, C., Melone, F., and Smith, R.E. (1994). "Modeling infiltration during complex rainfall sequences." *Water Resources Research,* 30(10), 2777–2784.

CRWMS M&O. (2000). *Yucca Mountain site description.* TDR–CRW–GS–000001, Rev 01 ICN 01. Civilian Radioactive Waste Management System Management and Operating Contractor, Las Vegas, Nv.

Day, W.C., Potter, C.J., Sweetkind, D., Dickerson, R.P., and San Juan,C.A. (1998). *Bedrock geologic map of the Central Block Area, Yucca Mountain, Nye County, Nevada.* U.S. Geological Survey Miscellaneous Investigations Series. Map I–2601.

EPRI. (2002). *Integrated Yucca Mountain safety case and supporting analysis.* EPRI 1003334. Electric Power Research Institute, Palo Alto, Ca.

Flint, A.L., Hevesi, J.A., and Flint, L.E. (1996). *Conceptual and numerical model of infiltration for the Yucca Mountain Area, Nevada.* USGS Water Resources Investigations Report (Draft). Yucca Mountain Project Milestone 3GUI623M.

Flint, A.L., Flint, L.E., Hevesi, J.A., and Hudson, D.B. (2001). "Characterization of arid land infiltration processes at Yucca Mountain, Nevada." *Flow and Transport through Unsaturated Fractured Rock,* 2nd Ed. D.D. Evans, T.C. Rasmussen, and T.J. Nicholson, eds. American Geophysical Union, Geophysical Monograph Series Volume 42, American Geophysical Union, Washington, DC, 135–149.

French, R.H., (1983). "Precipitation in southern Nevada." *Journal of Hydraulic Engineering* 109(7), 1023–1036.

Goodrich, D.C. (1990). *Geometric simplification of a distributed rainfall-runoff model over a range of basin scales*. Ph.D. Dissertation, Department of Hydrology and Water Resources, University of Arizona, Tucson, Az.

Hevesi, J.A., Flint, A.L., and Flint, L.E. (2003). *Simulation of net infiltration and potential recharge using a distributed-parameter watershed model of the Death Valley Region, Nevada and California.* USGS Water-Resources Investigations Report 03-4090. U.S. Geological Survey, Sacramento, Ca.

Kane, T.G. III, Bauer, D.G., and Martinez, C.M. (1994). *Streamflow and selected precipitation data for Yucca Mountain Region, Southern Nevada and Eastern California, Water Years 1986–90.* U.S. Geological Survey Open-File Report 93-438.994.

Kwicklis, E.M., and Rousseau, J.P. (1999). "Analysis of percolation flux based on heat flow estimated in boreholes." *Hydrogeology of the unsaturated zone, North Ramp Area of the Exploratory Studies Facility, Yucca Mountain, Nevada.* U.S. Geological Survey Water Resources Investigations Report 98-4050. J.P Rousseau, E.M. Kwicklis, and D.C. Gillies, eds.

Lane, L.J. (ed.), (1986). *Proceedings of the Rainfall Simulator Workshop, Jan. 14–15, 1985, Tucson, Az.* Society for Range Management, Denver, Co.

Lane, L.J., Romney, E.M., and Hakonson, T.E. (1984). "Water balance calculations and net production of perennial vegetation in the northern Mojave Desert ." *J. of Range Management* 37(1), 12–18.

Mohanty, S., McCartin, T.S., and Esh, D.W., coords. (2002). *Total-System Performance Assessment (TPA) Version 4.0 Code: Module description and user's guide.* CNWRA, San Antonio, Tx.

Mohanty, S., Codell, R., Menchaca, J., Janetzke, R., Smith, M., LaPlante, P., Rahimi, M., and Lozano, A. (2004). *System-level performance assessment of the proposed repository at Yucca Mountain using the TPA Version 4.1 Code.* CNWRA 2002-05, Rev 2.CNWRA, San Antonio, Tx.

Pabst, M.E., Beck, D.A., Glancy, P.A., and Johnson, J.A. (1993). *Streamflow and selected precipitation data for Yucca Mountain and vicinity, Nye County, Nevada, water years 1983–85.* U.S. Geological Survey Open-File Report 94-312.

Schmidt, M.R. (1988). *Classification of upland soils by geomorphic and physical properties affecting infiltration at Yucca Mountain, Nevada.* Master of Engineering Thesis, Colorado School of Mines, Golden, Co.

Simanton, J.R., Johnson, C.W., Nyhan, J.W., and Romney, E.M. (1986). "Rainfall simulation on rangeland erosion plots." *Proceedings of the Rainfall Simulator Workshop, Jan. 14–15, 1985, Tucson, Az.* L.J. Lane (ed.), Society for Range Management, Denver, Co., 11–17.

Simons, Li and Associates. (1982). *Engineering analysis of fluvial systems.* Simons, Li and Associates, Inc., Fort Collins, Co.

Smith, R.E., and Parlange, J.-Y. (1978). "A parameter-efficient hydrologic infiltration model." *Water Resources Research,* 14(3), 533–538.

Smith, R.E., Goodrich, D.C., and Woolhiser, D.A. (1990). "Areal effective infiltration dynamics for runoff of small catchments." *Transactions, 14th International Congress of Soil Science*, Kyoto, Japan, Vol. I, I.22–I.27.

Smith, R.E., Corradini, C., and Melone, F. (1993). "Modeling infiltration for multistorm runoff events." *Water Resources Research*, 29(1),133–144.

Smith, R.E., Goodrich, D.C., Woolhiser, D.A., and Unkrich., C.L. (1995). "Kineros–A KINematic runoff and EROSion model." *Computer Models of Watershed Hydrology*. V.P. Singh (ed.). Water Resources Publications, Highlands Ranch, Co., 697–732.

Squires, R.R., and Young, R.L. (1984). *Flood potential of Fortymile Wash and its principal southwestern tributaries, Nevada Test Site, southern Nevada*. U.S. Geological Survey Water Resources Investigations Report 83-4001.

Stothoff, S.A. (1995). *BREATH Version 1.1—Coupled flow and energy transport in porous media simulator description and user guide*. NUREG/CR–6333 and CNWRA 94-020.CNWRA, San Antonio, Tx.

USGS. (1995). *Water resources data Nevada water year 1995*. U.S. Geological Survey Water-Data Report NV–95–1.

USGS. (2001). *Simulation of net infiltration for modern and potential future climates*. ANL–NBS–HS–000032, Rev 00 ICN 02. Yucca Mountain Project, U.S. Geological Survey, Denver, Co.

Weltz, M.A., Arslan, A.B., and Lane, L.J. (1992). "Hydraulic roughness coefficients for native rangelands." *Journ. of Irrigation and Drainage Div*, ASCE, 118(5), 776–790.

Woolhiser, D.A., Smith, R.E., and Goodrich, D.C. (1990). *KINEROS, A kinematic runoff and erosion model: documentation and user manual.* U.S. Department of Agriculture, Agricultural Research Service, ARS–77, Southwest Watershed Research Center, Tucson, Az.

Woolhiser, D.A., Stothoff, S.A., and Wittmeyer, G.W.. (2000). "Channel infiltration in Solitario Canyon, Yucca Mountain, Nevada." *Journal of Hydrologic Engineering*, ASCE 5(3), 240–249.

Appendix II. Notation

The following symbols are used in this paper.

API = 7-day antecedent precipitation

BW = bottom width of a trapezoidal channel (m)

CV = coefficient of variation of saturated hydraulic conductivity

$DIST$ = soil hydraulic parameter

e_{ij} = excess infiltration for plane or channel i, storm j (mm)

E_i = total rainfall excess for plane or channel i (mm)

$\overline{E}_i$ = average annual rainfall excess for plane or channel i (mm)

F = output variable for sensitivity analysis

F_{Bij} = infiltration into bedrock for plane or channel i, storm j (mm)

F_{BPij} = potential bedrock infiltration for plane or channel i, storm j (mm)

f_{ij} = infiltration at ground surface for plane or channel i, storm j (mm)

G = net capillary drive (mm)

h = local depth of water (m)

K_S = hydraulic conductivity (mm/hr)

n = coefficient in Manning's equation

N = number of years of record

P = parameter varied for sensitivity analyses

P_{ij} = rainfall depth for plane or channel i, storm j (mm)

P_e = effective infiltrating wetted perimeter for a trapezoidal channel (m)

POR = porosity

P_w = wetted perimeter for a trapezoidal channel (m)

RE = relief of parallel, v-shaped micro-relief channels (mm)

S = sensitivity coefficient

SAT = initial relative saturation

SPA = spacing of parallel, v-shaped, micro-relief channels (m)

$SS1$ = side slope of trapezoidal channel

$SS2$ = side slope of trapezoidal channel

$THICK$ = depth of soil or channel alluvium thickness (mm)

LIST OF TABLES

Table 1
Rainfall Data and Simulated Runoff Volume and Channel Infiltration by Storm

File Name[a,b]	Day or Date	AP[c], mm	Depth, mm	Runoff Volume, mm	Channel Infiltration, mm
G3_87_1	201	8	26	0.0	0.22
G3_87_2	309, 310	20	34	0.0	0.31
G3_88_1	105, 106	2	38	0.02	0.42
G3_91_1	58, 58, 60	2	32	0.0	0.29
G3_92_1	5, 6	22	26	0.0	0.20
G3_92_2	37, 38	2	29	0.0	0.19
G3_92_3	40, 41, 42	29	28	0.0	0.18
G3_92_4	43, 44	57	29	0.0	0.21
G3_92_5	62, 63	2	28	0.0	0.18
G3_92_6	89, 90, 91	25	27	0.0	0.18
G3_92_7	342, 343	2	59	4.87	0.57
G3_93_1	16, 17, 18	32	28	0.0	0.18
G3_93_2	38	5	37	0.0	0.33
S18_94_1	12/24	1	24	0.0	0.20
S18_95_1	1/4–7	26	30	0.0	0.20
S18_95_2	1/21-26	10	87	11.35	0.63
S8_95_3	2/28	5	35	16.05	0.55
S8_3995b	3/9–11	41	80	0.0	0.23
	Annual Average			**3.59**	**0.58**

[a] G3 = USGS WX-3 raingage; S18 = SAIC #18 raingage; S8 = SAIC #8 raingage
[b] Middle portion of file name is last two digits of the year
[c] Antecedent precipitation

Table 2
Comparison of KINEROS2 Results with Data from Nearby USGS Streamgaging Stations

Station Number, Station Name	Area (km^2)	Storm of 1/26/95 Runoff Vol., mm	Storm of 1/26/95 Peak Rate, mm/hr	Storm of 3/9–11/95 Runoff Vol., mm	Storm of 3/9–11/95 Peak Rate, mm/hr
102512532, Pagany Wash #2	1.22	3.44e	—	24.3	3.24
102512533, Pagany Wash #1	2.12	0.01e	—	9.9	2.89
102512537, Split Wash below Quac Canyon	0.85	4.6e	—	8.7e	1.31
1025125356, Wren Wash at Yucca Mountain	0.59	6.6	—	10.8	5.13
Upper Split Wash, KINEROS2	0.25	11.35	2.78	16.1	3.18

e = estimated

Table 3
Dimensionless Sensitivity Coefficients for Storms S8_3995b and G3_88_1

S8_3995b	S_V	S_{CF}	S_{QP}	S_{FB}	S_{FBP}
THICK, soil	-1.47	0.517	-0.534	-0.088	0.275
K_S, Bedrock	-0.498	0.158	-0.214	0.584	0.186
API, 7-day	-0.035	-0.025	-0.071	—	—
DIST, soil	-0.459	-0.042	-0.409	0.425	0.510
G, soil	-0.031	0.017	-0.036	—	—
G3_88_1					
THICK, soil	-5.00	0.267	-5.00	-4.16	-0.438
K_S, Bedrock	-1.67	0.116	-0.143	0.369	0.002
API, 7-day	0.833	0.058	0.807	—	—
DIST, soil	-5.00	-0.116	-6.429	-1.34	0.151
G, soil	-0.833	0.140	0.571	—	—

LIST OF FIGURES

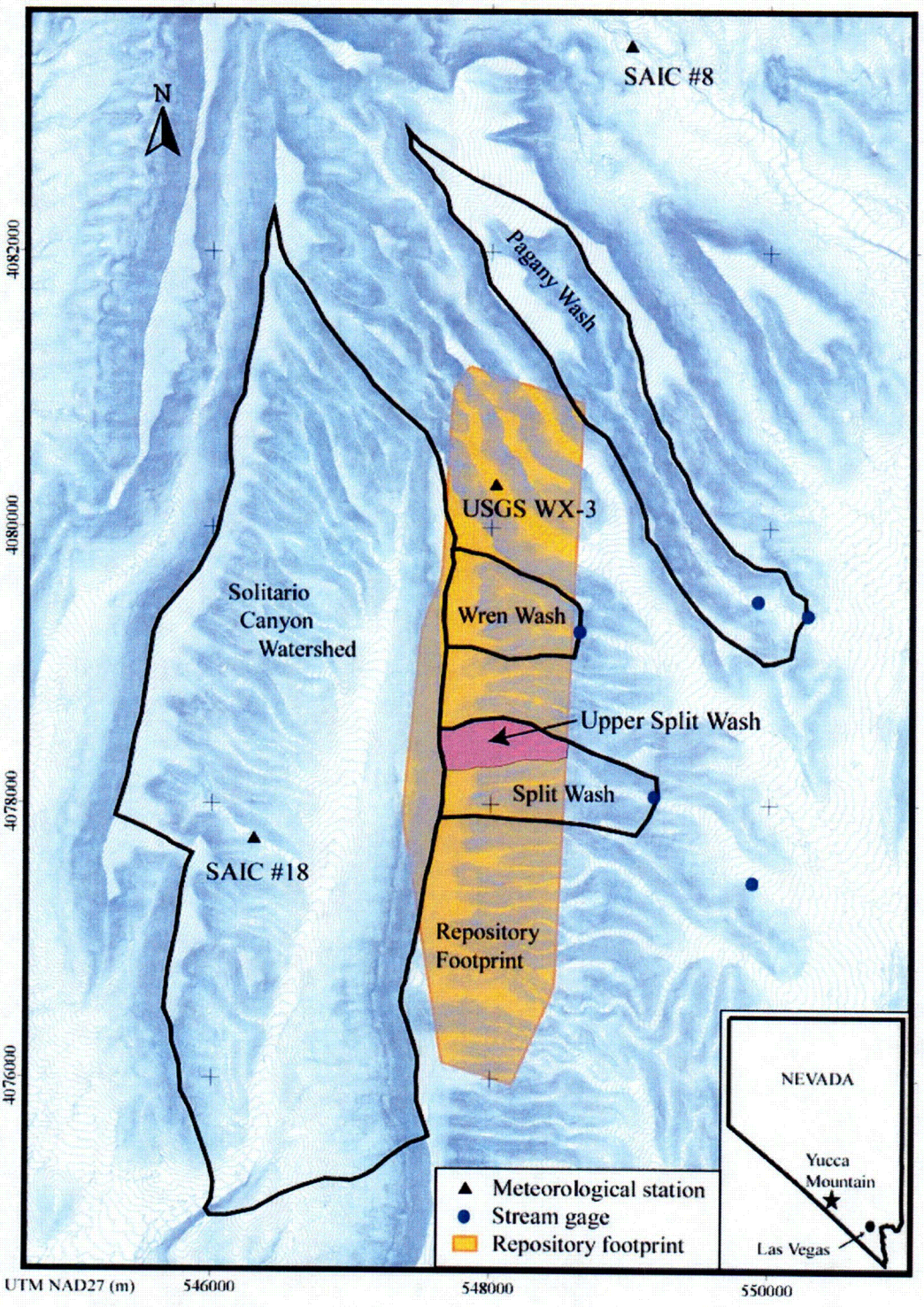

Figure 1. Location Map of Upper Split Wash Showing Stream Gaging Stations and Raingages

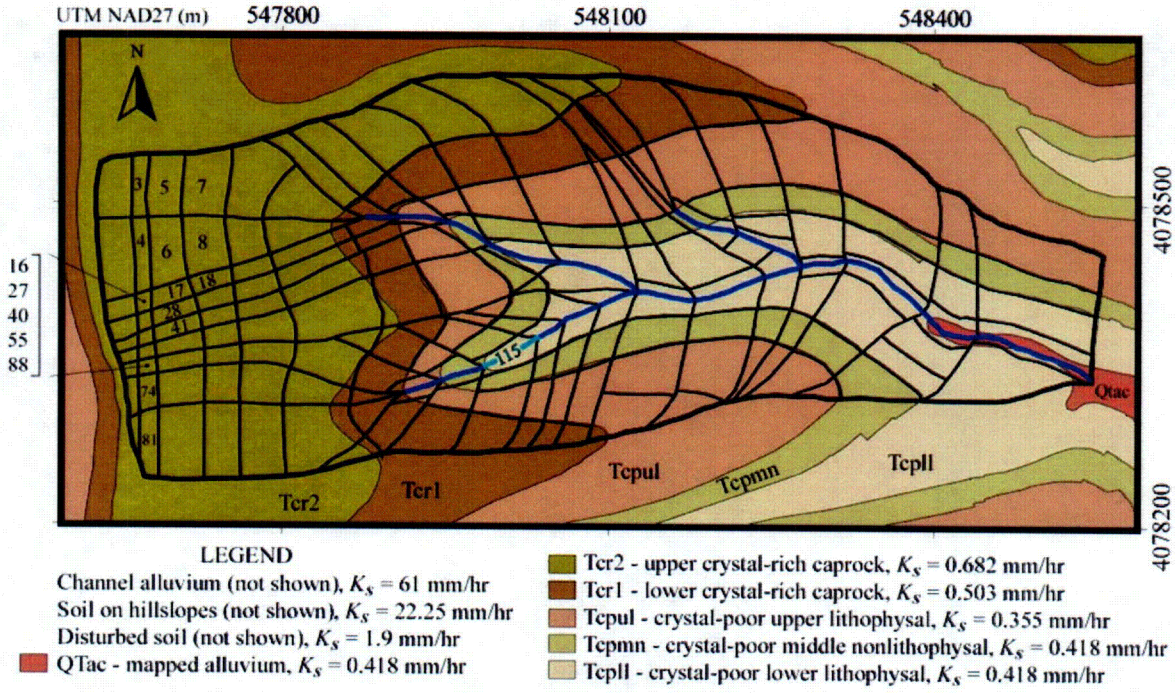

Figure 2. Map Showing Bedrock Geology, Plane and Channel Elements, and Selected Element Numbers

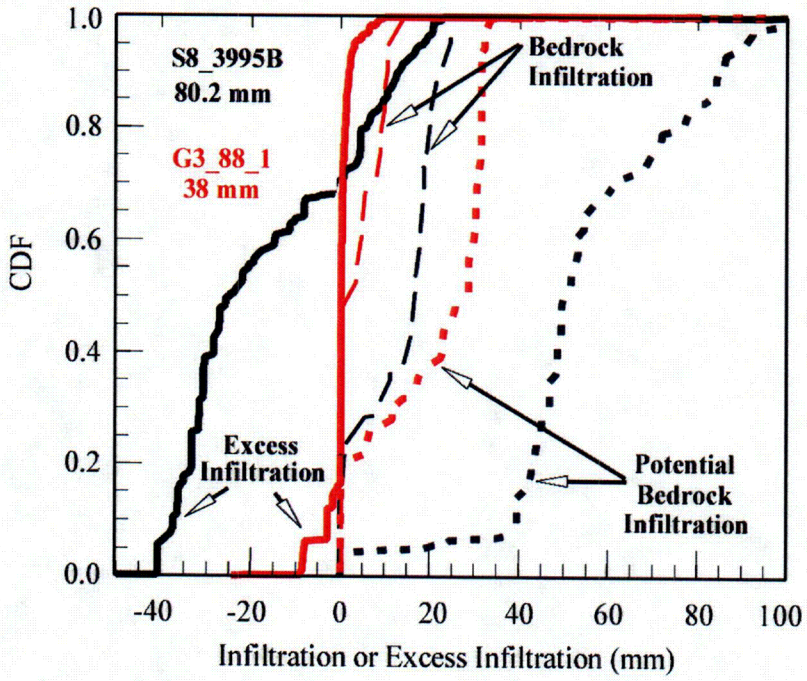

Figure 3. Cumulative Distribution Functions of Excess Infiltration, Bedrock Infiltration, and Potential Bedrock Infiltration for Precipitation Events G3_88_1 and S8_3995B

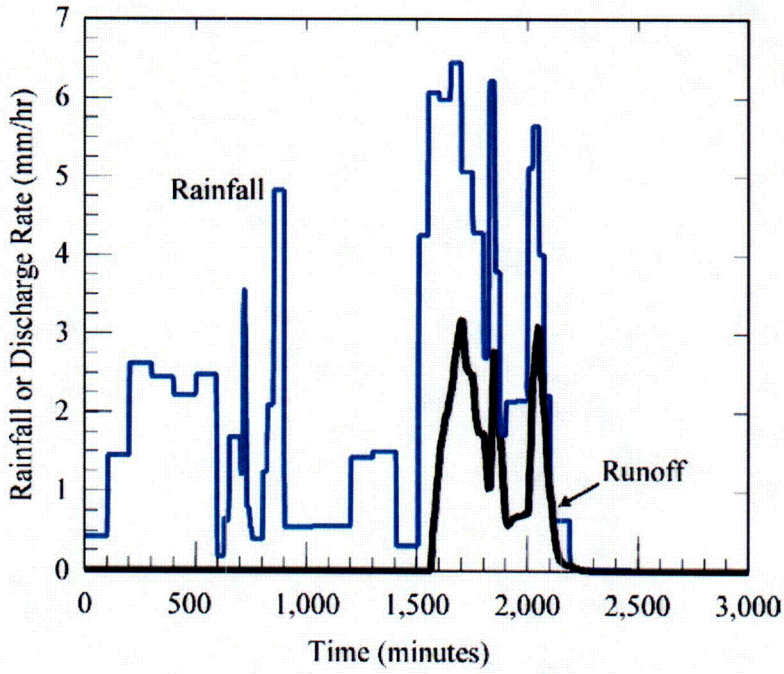

Figure 4. Rainfall Hyetograph and Runoff Hydrograph for the Event S8_3995b

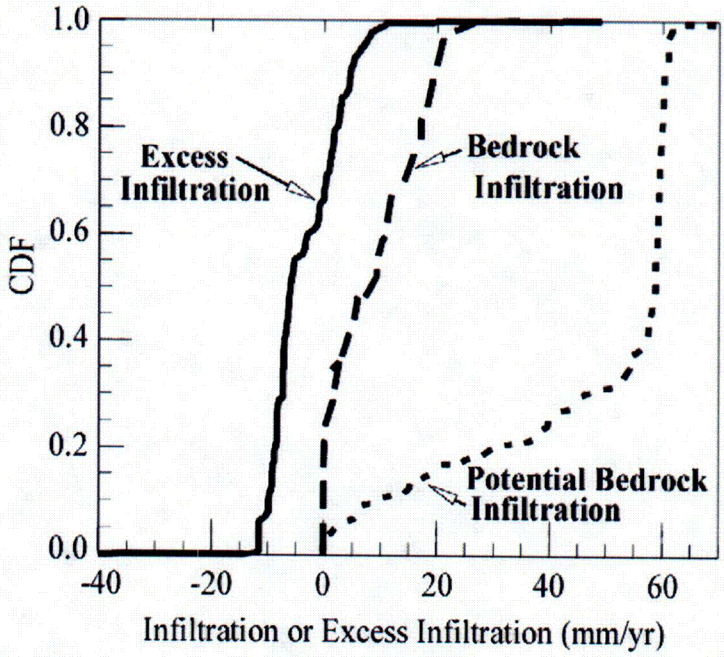

Figure 5. Cumulative Distribution Functions of Average Annual Excess Infiltration, Bedrock Infiltration, and Potential Bedrock Infiltration

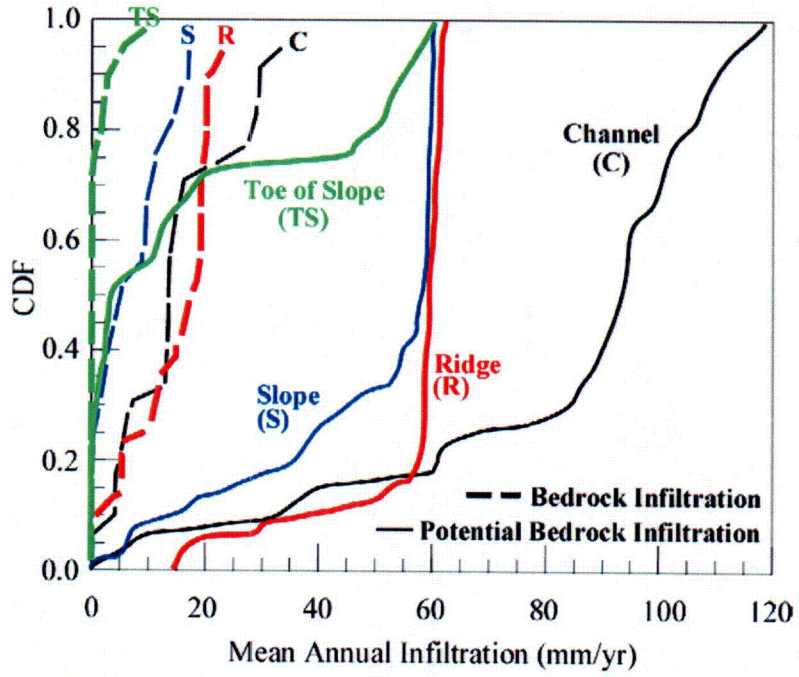

Figure 6. Cumulative Distribution Functions of Average Annual Bedrock Infiltration, and Potential Bedrock Infiltration for Three Hillslope Elements and Channels

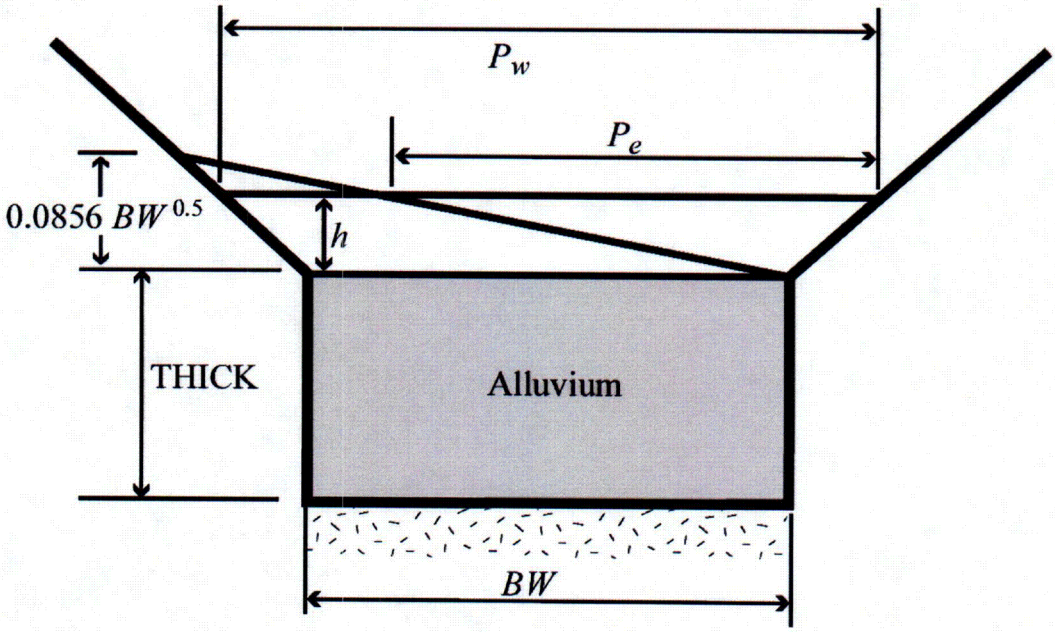

Figure 7. Channel Cross Section

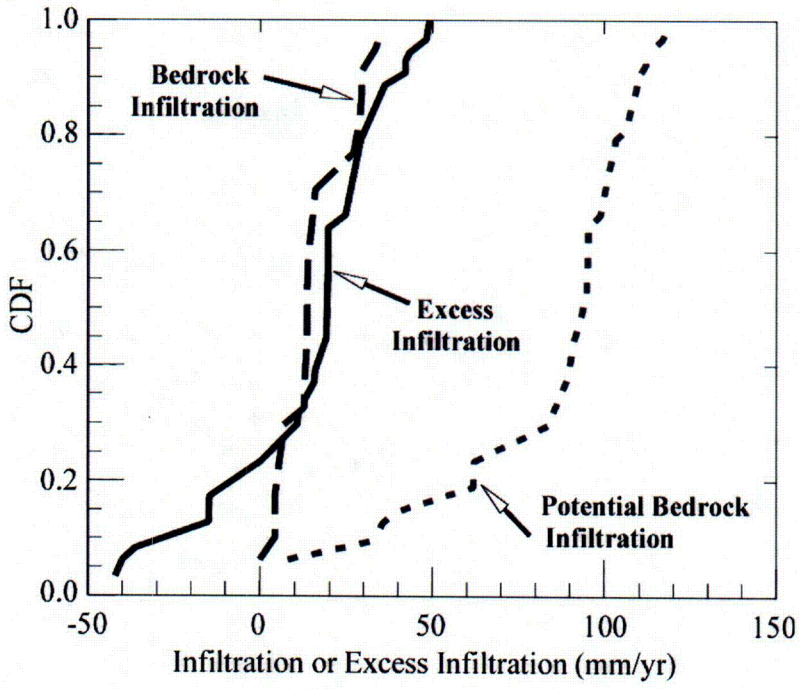

Figure 8. Cumulative Distribution Function of Annual Average Potential Infiltration Into Bedrock Below Channels